

Supplementary information

# Porous silicon-nanowire-based electrode for the photoelectrocatalytic production of hydrogen

Jingxian Wang<sup>1,2</sup>, Caroline Keller<sup>1,3</sup>, Marc Dietrich<sup>1,4</sup>, Pascal Gentile<sup>4</sup>, Stéphanie Pouget<sup>5</sup>, Hanako Okuno<sup>5</sup>, Mohamed Boutghatin<sup>6</sup>, Yan Pennec<sup>6</sup>, Valérie Reita<sup>7</sup>, Duc N. Nguyen<sup>2,8</sup>, Hannah Johnson<sup>9</sup>, Adina Morozan<sup>2</sup>, Vincent Artero<sup>2,\*</sup>, Pascale Chenevier<sup>1,\*</sup>

<sup>1</sup> Univ. Grenoble Alpes, CEA, CNRS, IRIG, SyMMES, 38000 Grenoble, France

<sup>2</sup> Univ. Grenoble Alpes, CEA, CNRS, IRIG, Laboratoire de Chimie et Biologie des Métaux, 38000 Grenoble, France

<sup>3</sup> Univ. Grenoble Alpes, CEA, LITEN, DEHT, 38000 Grenoble, France

<sup>4</sup> Univ. Grenoble Alpes, CEA, Grenoble-INP, IRIG, PheLIQS, 38000 Grenoble, France

<sup>5</sup> Univ. Grenoble Alpes, CEA, IRIG, MEM, 38000 Grenoble, France

<sup>6</sup> Univ. Lille CNRS UMR 8520 – IEMN – Institut d'Electronique de Microélectronique et de Nanotechnologie Lille F-59000, France

<sup>7</sup> Univ. Grenoble Alpes, CNRS, Institut Néel, 38000 Grenoble, France

<sup>8</sup> University of Science and Technology of Hanoi, Vietnam Academy of Science and Technology, Hanoi 100000, Vietnam

<sup>9</sup> Toyota Motors Europe, Brussels, Belgium

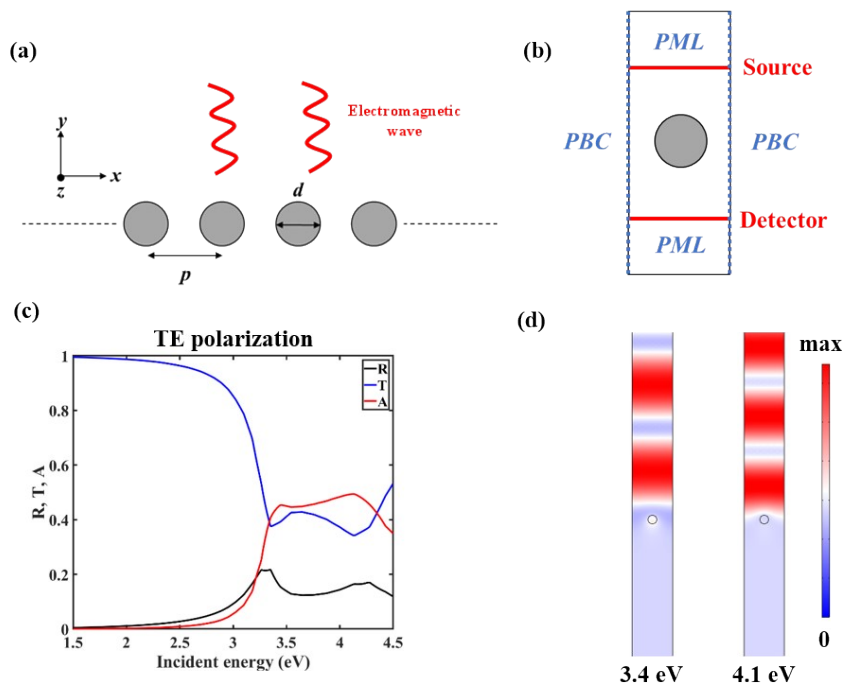


Figure S1. Calculation of the interaction of light with SiNWs. (a) 2D schematic representation of the one-dimensional periodic array of SiNWs of period  $p$  embedded in dichloromethane solution. (b) Unit cell used for the Finite Element Method (FEM) calculation, applying periodic boundary (PBC) along  $x$  and perfect matching layers (PML) along  $y$ . (c) Calculated  $R$  (black),  $T$  (blue), and  $A$  (red) for TE polarization with the geometrical parameters  $d = 13$  nm and  $p = 60$  nm. (d) Map of the electric field modulus  $E$ , at the energy 3.4 eV and 4.1 eV.

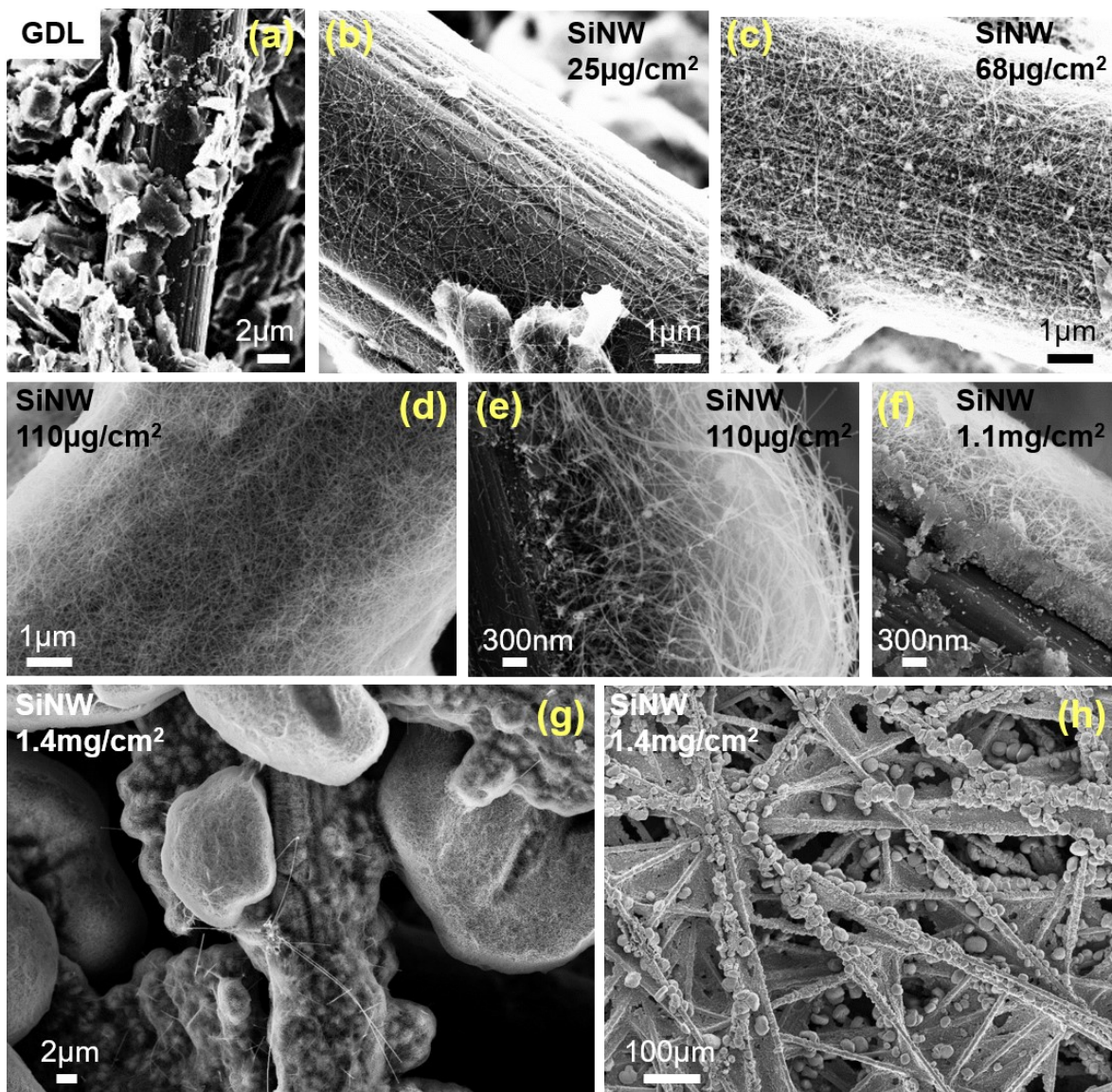


Figure S2. SEM images of PCS-SiNW with 13 nm SiNWs at different areal densities of (a) 0, (b) 25, (c) 68, (d-e) 110  $\mu\text{g}/\text{cm}^2$  and (f) 1.1 and (g-h) 1.4  $\text{mg}/\text{cm}^2$ .

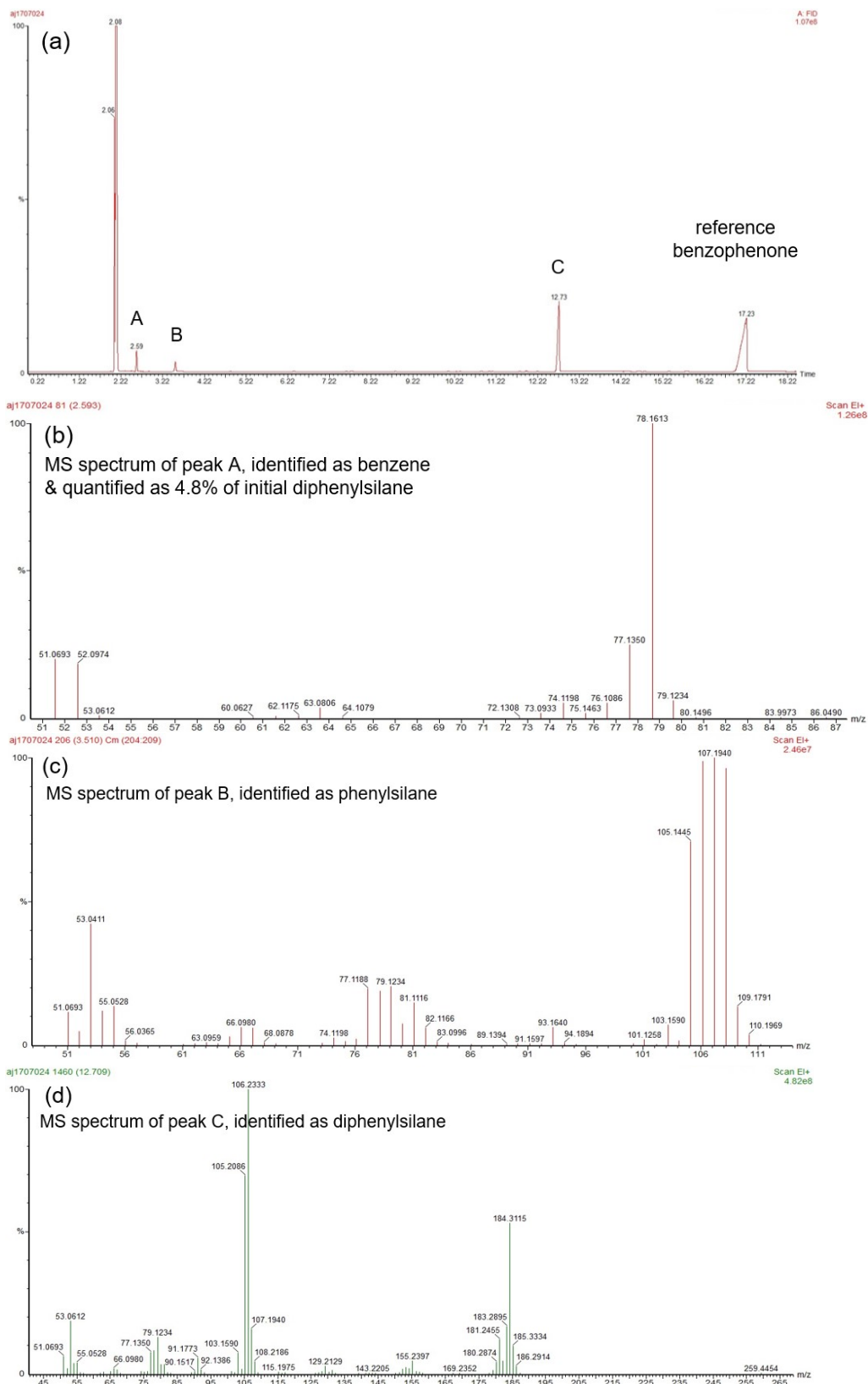


Figure S3. Detection of benzene in SiNW growth by-products by Gas chromatography (GC) and mass spectroscopy (MS): (a) GC spectrum of a solution of SiNW growth sub-products, to which a reference amount of benzophenone was added for quantification of benzene following a standard. (b), (c) and (d): MS spectra of the peaks A, B and C labeled in (a) respectively.

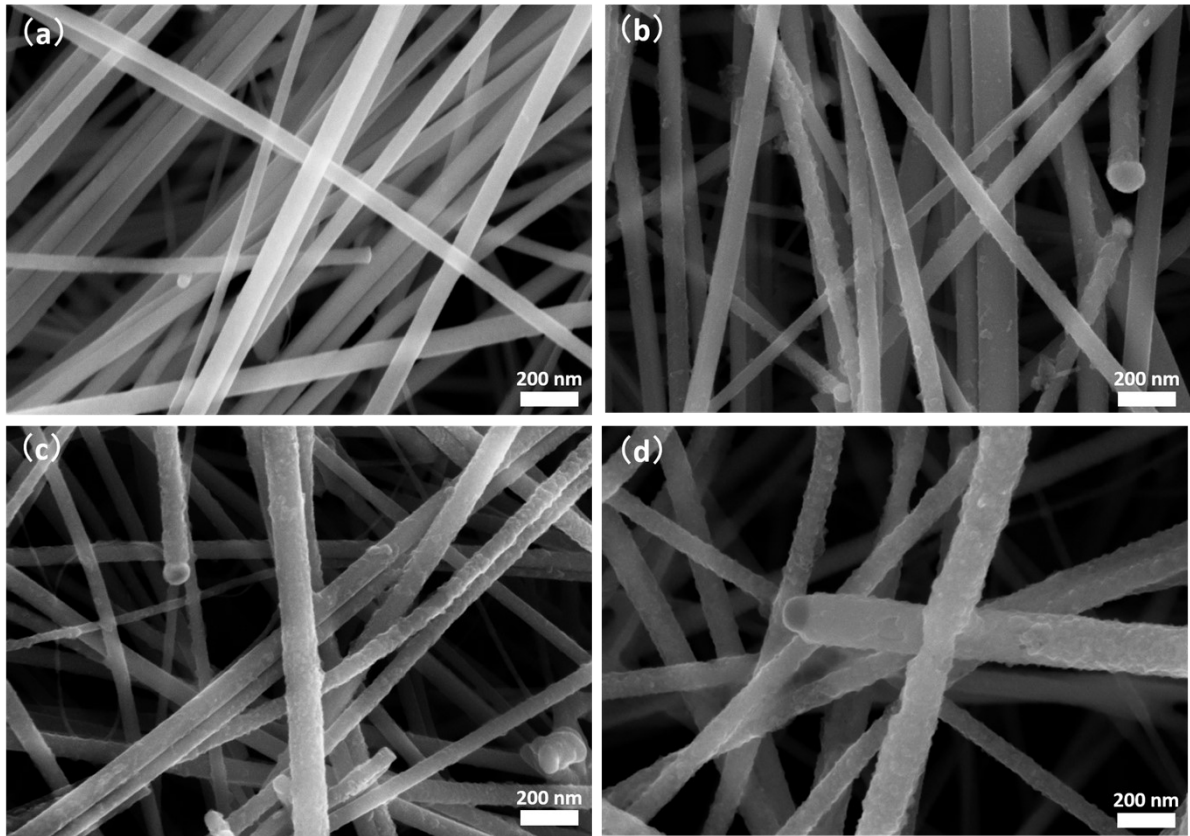


Figure S4. SEM images of (a) 48nm-SiNWs, 48 nm-SiNWs-MoS<sub>x</sub> with (b)  $\Delta Q = 1 \text{ mC/cm}^2$ , (c)  $\Delta Q = 6 \text{ mC/cm}^2$  and (d)  $\Delta Q = 50 \text{ mC/cm}^2$ .

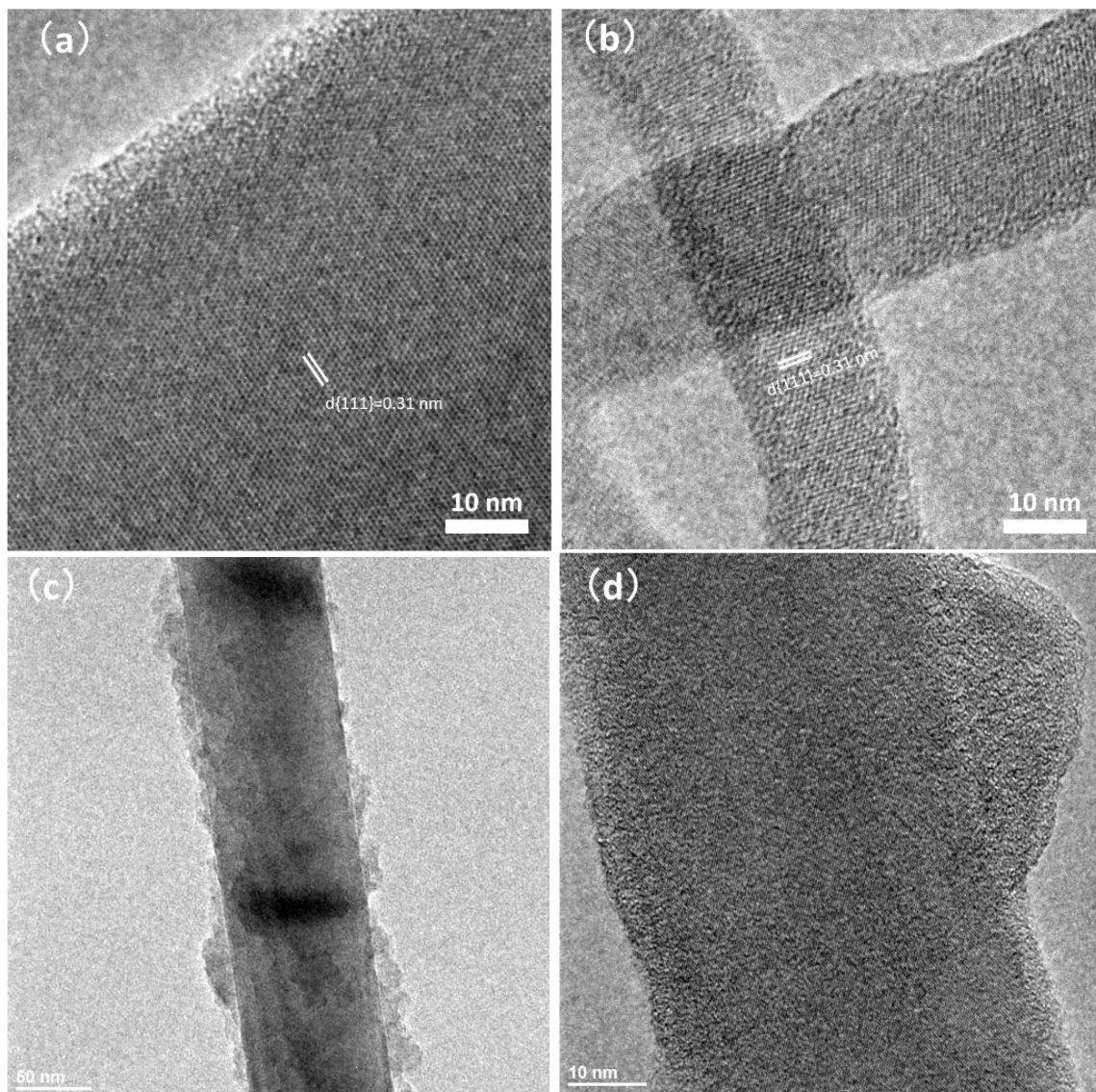


Figure S5: TEM images of (a) 48 nm-SiNWs and (b) 13 nm-SiNWs in high resolution; (c) SiNW-MoS<sub>x</sub> at low magnification and (d) in high resolution.

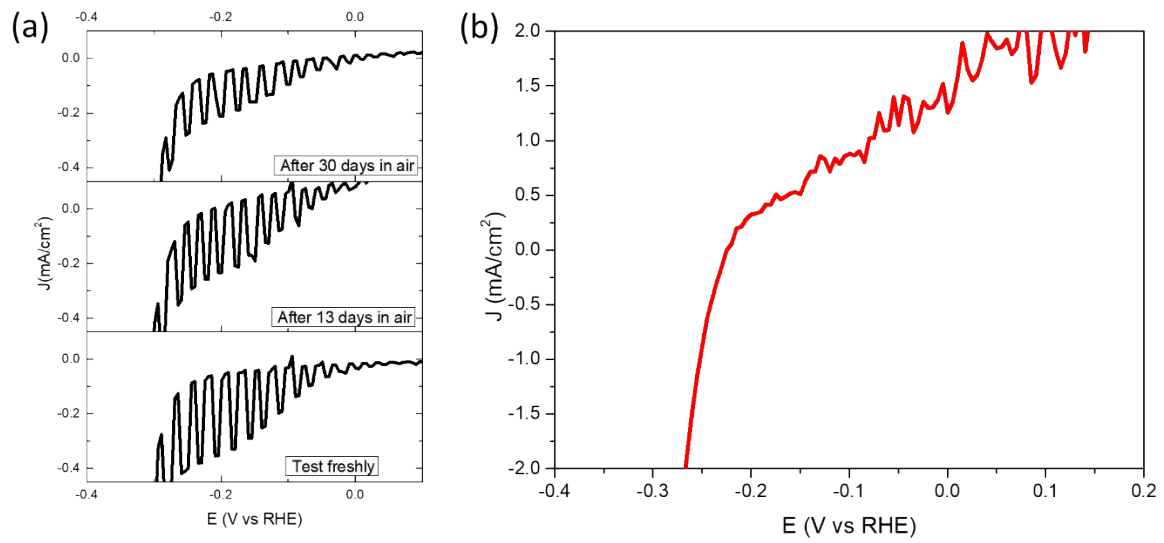


Figure S6: (a) PEC of PCS-SiNW-MoS<sub>x</sub> photocathodes with a SiNW diameter of 48 nm when MoS<sub>x</sub> is deposited just after SiNW growth, or when delaying MoS<sub>x</sub> deposition for 13 and 30 days; (b) PEC of PCS-SiNW<sub>CVD</sub>-MoS<sub>x</sub> for SiNWs grown by CVD under chopped illumination.

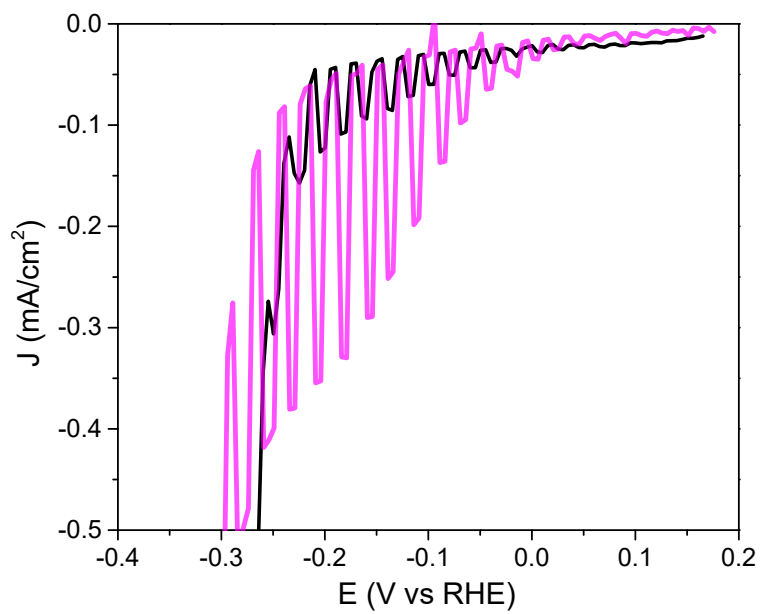


Figure S7: PEC performance for PCS-SiNW-MoS<sub>x</sub> photocathodes with 13nm- (black) and 48nm-SiNWs (magenta).

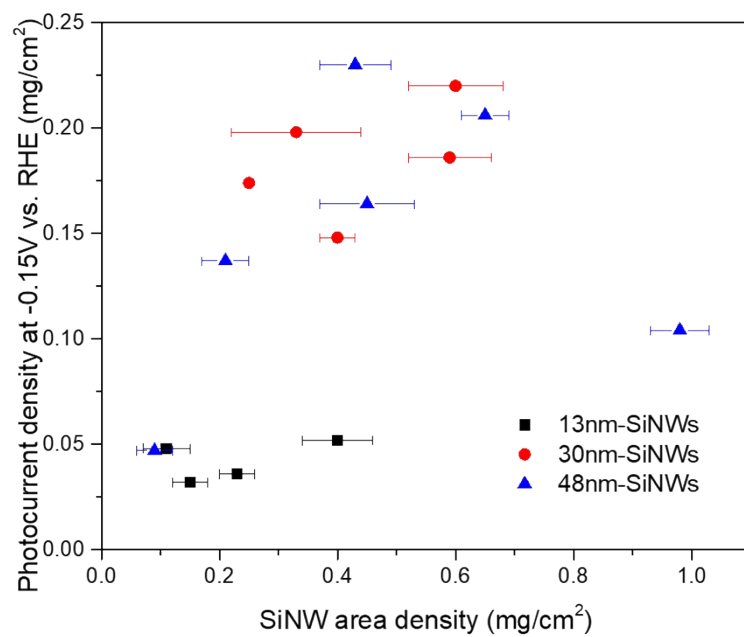


Figure S8: Photocurrent density of PCS-SiNW-MoS<sub>x</sub> (with different nanowire diameters) at -0.15V vs. RHE as a function of SiNWs areal density.

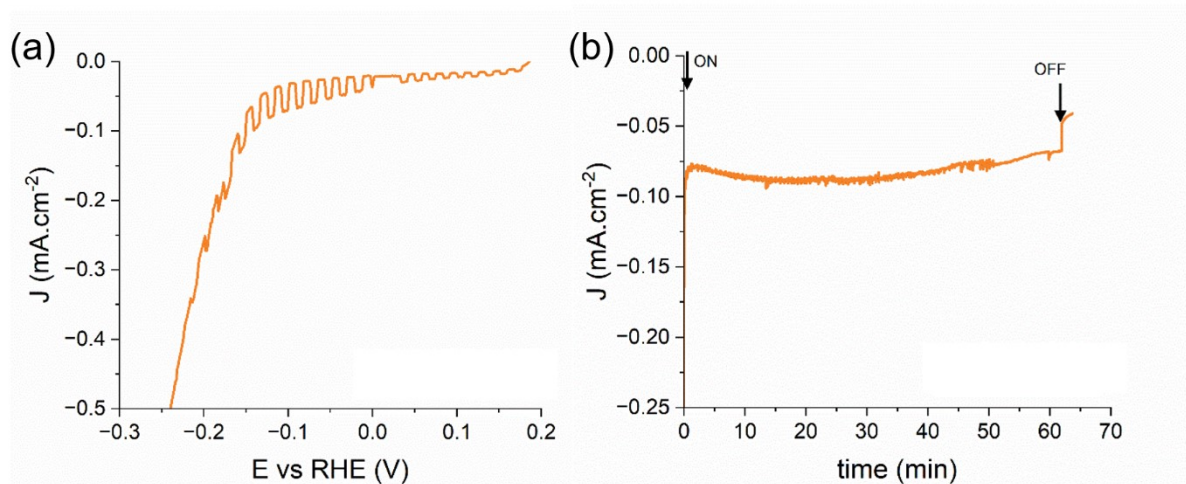


Figure S9: Photoelectrocatalysis performance of PCS-SiNW-MoS<sub>x</sub> with 48 nm-SiNWs (a-MoS<sub>x</sub> deposition:  $\Delta Q = 6 \text{ mC/cm}^2$ ) in 0.5 M H<sub>2</sub>SO<sub>4</sub> electrolyte, second sample similar to the one used for Figure 6. (a)  $J$ - $V$  curve of PCS-SiNW-MoS<sub>x</sub> electrodes under chopped illumination. (b) Chronoamperometry at -0.15 V vs. RHE under illumination in a tightly closed system.